J. Fluid Mech. (1971), *vol.* 48, *part* 4, *pp.* 703–719
Printed in Great Britain

Convection experiments with electrolytically heated fluid layers

By E. W. SCHWIDERSKI AND H. J. A. SCHWAB
U.S. Naval Weapons Laboratory, Dahlgren, Va.

(Received 31 August 1970 and in revised form 26 April 1971)

Convection experiments described by Tritton & Zarraga (1967) with electrolytically heated fluid layers were renewed in order to investigate the reported phenomena, which were hitherto unknown and which contradicted a corresponding theory of Roberts. While the apparatus was essentially unchanged, provisions were incorporated to study the possible influence of several flow and equipment parameters on the convection pattern. With the exception of the temperature dependence of the electric conductivity, the new experiments displayed no essential effects of the convection parameters. Experiments with shallow fluid layers revealed a clear co-orientation of the convection flows with the electric current and a strong time dependence of the hexagonal patterns. Experiments with deeper fluid layers exhibited a considerably diminished time and direction dependence of the convection flow, and a significant reduction of the dilation of the cells. Based on these observations, it is concluded that no drastic differences between theory and experiments, and between internal and external heating, exist, provided the heating is sufficiently uniform.

1. Introduction

Tritton & Zarraga (1967) described convection experiments with electrically conducting fluid layers under gravity, which were internally heated by an alternating current and cooled from above. The reported convection pattern conflicted with a corresponding theory of Roberts (1967), and with other theories and experiments of similar flows, at several major points.

(i) Tritton & Zarraga observed a more or less regular hexagonal convection pattern with some indication of change toward rolls at high Rayleigh numbers specifying the heating. Roberts's analysis found all hexagonal flows as unstable at lower Rayleigh numbers. Only roll currents are neutrally (marginally) stable, and, hence, should be exclusively observed. While the rolls maintain their neutral stability for all Rayleigh numbers, the hexagonal motions become increasingly stable with growing Rayleigh numbers and should be physically preferred.

In the classical Bénard problem (where the fluid is heated from below and cooled from above) very regular hexagonal cells were observed. However, when the analysis of Schlüter, Lortz & Busse (1965) revealed only Bénard convection in rolls as stable, renewed experiments by Somerscales & Dropkin (1966) and by Krishnamurti (1968) verified the theoretical results. The earlier hexagonal

motions were attributed by Palm (1960), Busse (1962), Segel (1965), Krishnamurti (1968), Davis & Segel (1968), Somerscales & Dougherty (1970), and others, to temperature dependent fluid parameters.

(ii) The radius of the hexagonal cells observed by Tritton & Zarraga was comparable with the fluid-layer depth at low Rayleigh numbers, but increased to five times this depth as the heating was increased. In Roberts's theory, the neutrally stable wavelength of the roll convection decreases slightly with increasing Rayleigh numbers. The same remains true for the preferred hexagonal flow within its stable range at large Rayleigh numbers.

In Bénard convection, no such drastic dilations of the preferred cells have been revealed by theory or experiment. Only minor wave-number changes have been reported by Koschmieder (1966, 1969), Nield (1968), Chen & Whitehead (1968), Segel (1969), and others. These variations have been explained by the physical properties of the top, bottom, and side boundaries, and by the initial (hysteresis) conditions. In this respect, one may also compare the experiments of Snyder (1969) with the theory of Davey, DiPrima & Stuart (1968) concerning Taylor vortices between rotating cylinders (which are similar to convection with internal heating).

(iii) Though the experiments of Tritton & Zarraga and the theory of Roberts found physically realizable motions in hexagons at different Rayleigh and wave-numbers, they agreed in the direction of the circulation. If hexagonal convection is possible, the fluid should be falling at the centre and rising at the walls of the cell (down-hexagons). However, this is in disagreement with the earlier observations of Bénard convection in hexagons where the fluid is ascending at the centre and descending at the walls of the cell (up-hexagons), at least at comparable Prandtl numbers. Again, newer investigations indicate the possibility of down-hexagons in the case of variable fluid parameters.

Neither Tritton & Zarraga nor Roberts offered a satisfactory explanation for their inconsistencies, and for the deviations from other flow phenomena. The former attempted an heuristic explanation for the instability of small hexagonal cells. In their opinion, owing to the internal heating, strong buoyancy forces may develop in the central regions of vanishing convection, and disrupt the small cells. Since the regions of vanishing motion are definitely larger in the elongated cells, the same argument would disallow their existence. In fact, if the conjecture of Tritton & Zarraga is correct, one might not expect a steady state at all. However, Tritton & Zarraga did not mention any transient features of their photographed flow patterns.

The unanswered questions raised by the experiments of Tritton & Zarraga and the theory of Roberts warrant a re-investigation. As a first step, the authors decided to repeat the experiments with the following objectives:

(*a*) To eliminate or improve all undesirable imperfections of the apparatus, which could possibly affect the convection pattern.

(*b*) To evaluate the influence of unremovable imperfections or idealizations of the apparatus on the motion.

(*c*) To study the evolution of the convection with respect to time and history.

(*d*) To derive a model, and, perhaps, a lead for an appropriate theory.

The last two objectives are of particular significance for all bifurcation problems of viscous flow, such as the Rayleigh convection and Taylor vortex flow. Recent theoretical and experimental studies of Schlüter *et al.* (1968), Davey *et al.* (1968), Davis & Segel (1968), Snyder (1969), Somerscales & Dougherty (1970), and others, seem to indicate that the bifurcation solutions of the Navier–Stokes equations are degenerate with respect to their uniqueness. Beyond certain critical dynamical parameters, the equations of viscous flow may yield many laminar and steady-state solutions, and many of them appear to be stable against small perturbations. Moreover, even though a solution may be stable against small perturbations, it may be unstable against large disturbances. In this connexion, the papers by Busse (1962), Joseph & Shir (1966), Krishnamurti (1968), and Fife & Joseph (1969), concerning subcritical convection, may be quoted as examples.

2. Experimental arrangement

The apparatus used was essentially the same as that described by Tritton & Zarraga (1967). However, the design of the cooling plate was changed in two ways. First, the subdivision into separated channels for the cooling water was abandoned. This was desirable to exclude any arguments about the periodicity of cooling conditions across the fluid layer which could interfere with the periodic temperature distribution caused by the convection. Secondly, for the same reason Teflon was used for the electrical insulation between the cooling plate and the convecting fluid. With Teflon, one can obtain a very thin layer with little variation in thickness.

Figure 1 is a scale drawing of the equipment. The fluid is shown as the dotted area. It is confined between the cooling plate on the top and the insulating plates on the bottom. The fluid is aqueous zinc sulphate solution of specific gravity of about 1·05 g cm^{-3}. The flow and the resulting cell patterns are made visible by polystyrene beads suspended in the fluid as described by Tritton & Zarraga. The concentration of the beads in the solution was about 1 %. If the bead concentration in the fluid is made higher (which would enhance the visibility of the flow pattern), the flow development of the convection is slowed down. The concentration of the $ZnSO_4$ solution was adjusted for optimum results in pattern visibility. The plate forming the bottom of the convective space is shown as glass, but it could be replaced by a Plexiglass plate of identical dimensions for a study of the influence of its thermal conductivity on the cell pattern. The tank in which the whole equipment rests is made of lucite.

The cooling plate is aluminium. A thin layer of cooling water runs through it. Two relatively large water tanks are attached at the opposite ends of the cooling plate to ensure a constant pressure difference along the plate over its whole width. Thus, the water will run at the same speed everywhere across the plate and achieve a uniform cooling.

In figure 1 the thickness of the Teflon layer electrically insulating the convecting fluid from the cooling plate is exaggerated, in order to show it. The actual layer is 0·1 mm thick as determined by capacity measurements. It varies by about ± 3 % over the area of the plate. After the cooling plate was completed, the

Teflon layer was found to withstand a voltage of 2000 V(d.c.) without breakdown. Since the maximum voltage that could ever be applied across the layer in the experiment was below 400 V, the layer could be reduced in thickness considerably. This should be done in any future experiments, in order to reduce the undesired thermal insulation introduced by the Teflon layer between the fluid and the cooling plate. For an investigation of the influence of this thermal insulation some experiments were made with increased insulation. The additional insulation was achieved by one or more layers of insulating tape attached to the Teflon layer.

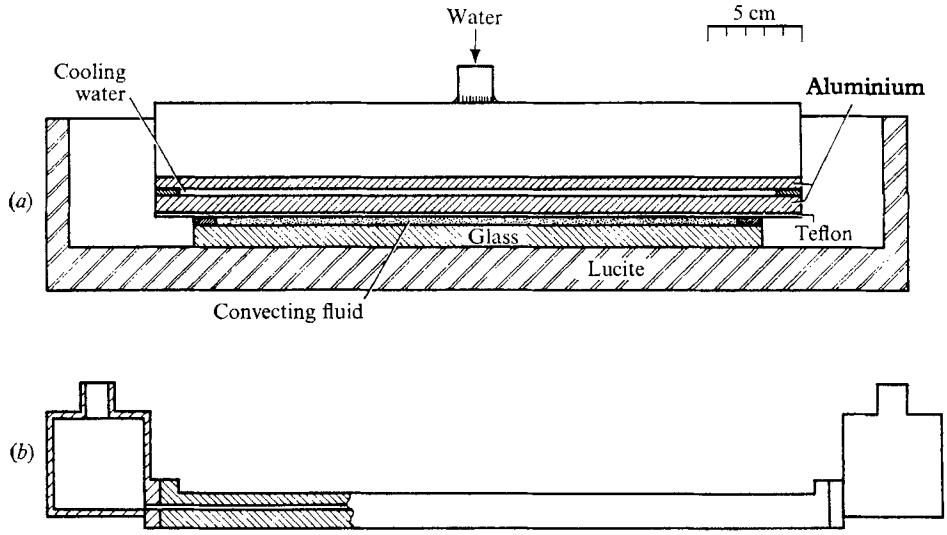

FIGURE 1. Scale drawing of the experimental equipment. (*a*) Cross-section of the assembled equipment. (*b*) Cooling plate, turned by 90° with respect to position in (*a*).

The walls of the tank that contained the convecting fluid were made of lucite, and were 0·44 cm high. The actual height of the convecting fluid layer was 0·46 cm, because a strip of insulating tape was attached to the Teflon layer where it rested on the walls of the tank. This tape was used to protect the Teflon layer from damage by polystyrene beads, which were caught between the tank walls and the cooling plate when the tank was filled. The beads are very hard and impress marks into the Teflon coat, which can eventually lead to electrical breakdown of the insulation. Because of beads being caught this way, the fluid-layer height had an uncertainty of $+0{\cdot}4$ mm. Compared to this, the deviation from flatness of the bottom and the cooling plate was negligible. As is reported in § 6, the walls of the tank were also increased to 0·9 cm to achieve a fluid depth of 0·92 cm.

The convecting fluid was heated electrolytically by a 60 Hz alternating current. Two zinc electrodes were attached to two opposite walls of the tank along its whole length. The direction of the electrical current could be selected either parallel or vertical to the direction of the flow of the cooling water, the temperature of which was variable. Finally, the horizontal size of the convection space was adjustable by means of a lucite strip, which could be inserted anywhere in the convection space to provide an additional boundary.

3. Rayleigh number and average temperature rise

The definition of the Rayleigh number for internal heat generation is

$$R = \frac{\alpha g h d^5}{\nu \kappa k}; \tag{1}$$

here α is the coefficient of thermal expansion, g the acceleration due to gravity, d the depth of the fluid layer, ν the kinematic viscosity, κ the thermometric conductivity, and k the thermal conductivity of the fluid. The heat generation per unit volume and time h needs some more elaboration. Since the heat is generated by an electric current, it can be written as

$$h = \mathbf{J}.\mathbf{E} = \sigma E^2; \tag{2}$$

where $\mathbf{J}$ is the current density, $\mathbf{E}$ the electric field strength in the fluid, and σ its electric conductivity. The value of σ is a function of temperature T, which can be approximated by

$$\sigma = \sigma_0[1 + \beta(T - T_0)], \tag{3}$$

where σ_0 is the conductivity at a reference temperature T_0 and β the temperature coefficient. Figure 2 shows measured values of σ and their representation by a straight line according to (3). From these values one obtains $\beta = 0{\cdot}022\,°\mathrm{C}^{-1}$.

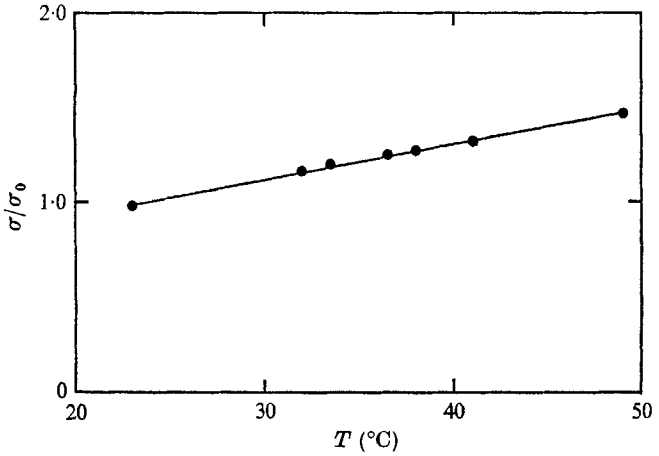

FIGURE 2. Electric conductivity of $ZnSO_4$ solution as a function of temperature. $\sigma = \sigma_0(1 + 0{\cdot}022\,\Delta T)$, $\sigma_0 = 23 \times 10^{-3}$ mho cm^{-1} at $T_0 = 24$ °C.

With the electric conductivity depending so strongly on temperature, both σ and E will vary as a function of position in the fluid, according to the temperature distribution introduced by the convection. For the value of h entering in the Rayleigh number it seems most convenient to use an average value,

$$\bar{h} = \overline{\sigma E^2}. \tag{4}$$

Of course, $\bar{h}$ can be related to the total heat input H:

$$\bar{h} = \frac{H}{abd} = \frac{VI}{abd}, \quad H = V \times I; \tag{5}$$

here I is the total electric current through the fluid, and V the total voltage across the fluid. The letter a denotes the length of the convection space in the direction of the electric current, and b the width vertical to it. With $a = 27{\cdot}3$ cm, $b = 28{\cdot}0$ cm, $d = 0{\cdot}46$ cm, one obtains

$$\bar{h} = \frac{VI}{352} \text{ watts cm}^{-3}, \tag{6}$$

where V is measured in volts and I in amperes.

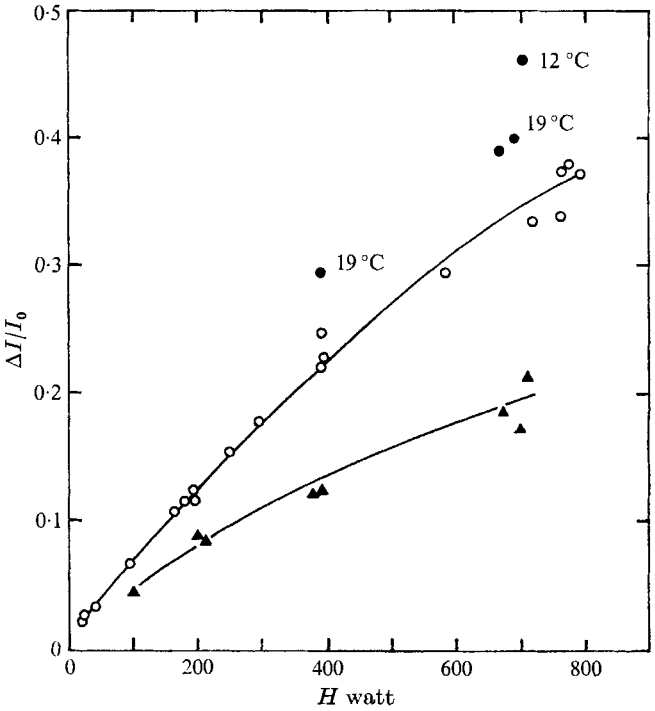

FIGURE 3. Increase of the electric current through the fluid between the beginning of an experiment and stabilization. The temperatures refer to the cooling water temperature T_c ($d = 0{\cdot}46$ cm). ●, glass, various T_c; ○, glass, 24 °C; ▲, Plexiglass, 24 °C.

At the beginning of each experiment the temperature of the fluid in the convection space is equal to the temperature of the cooling water. When power is applied, the fluid will gradually heat up until an equilibrium is reached. This increase in temperature causes an increase in conductivity, which in turn will cause H to change. For experimental convenience, the fluid was heated by applying a constant voltage and allowing the current to adjust itself. For the value of total heat input H, which is quoted in this paper, the final current used was that reached after an initial transient period. The Rayleigh number is defined accordingly. For a cooling water temperature $T_c = 24$ °C, one obtains

$$R \approx 162H, \tag{7}$$

where H is entered in watts.

Figure 3 shows measured values of

$$\frac{\Delta I}{I_0} = \frac{I_{\text{end}} - I_0}{I_0} \tag{8}$$

as a function of power input H, where I_0 is the initial current at time $t = 0$ and I_{end} the current after it has stabilized. One can see that $\Delta I/I_0$ depends on the thermal properties of the tank bottom. It also depends on temperature. The cooling water temperature T_c for the curves of figure 3 was 24 °C. A typical variation of $\Delta I/I_0$ with cooling water temperature is also shown by some points in figure 3.

If the horizontal variation of σ in the fluid is not too strong, the increase in total current is proportional to the increase in average conductivity, which is related to the fluid temperature by (3). By using this relation an approximate value of the average temperature increase in the fluid can be determined. The changes of temperature and conductivity computed from $\Delta I/I_0$ are values averaged over the fluid volume. Since the cooling temperature is fixed at T_c the difference,

$$\overline{\Delta T} = \bar{T} - T_c, \tag{9}$$

is the average temperature increase caused by the applied power. This value is shown in figure 4 by the solid curves.

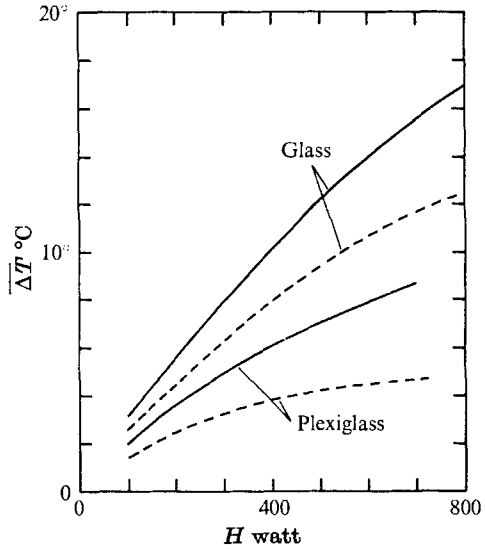

FIGURE 4. Approximate increase of the mean temperature in the fluid. – – – –, temperature difference on Teflon layer and aluminium subtracted (d = 0·46 cm). T_c = 24 °C.

Not all of this temperature increase is due to building up a temperature profile in the fluid to remove the heat created in it. A fraction of $\overline{\Delta T}$ represents a temperature drop on the insulation and metal layers of the cooling plate. With the thermal conductivities of Teflon and aluminium being 0·0006 and 0·55 cal sec^{-1} cm^{-1} °C^{-1}, respectively, the temperature difference across these layers can be

estimated under the assumption that all heat generated in the fluid leaves through the cooling plate. The deduction of this amount from the measured mean temperature rise results in the broken line curves in figure 4. This gives the mean temperature increase in the fluid caused by the temperature gradients inside the fluid.

The fraction of the total heat that leaves the fluid through the cooling plate can also be estimated. Under the assumption of a linear vertical distribution of the horizontally averaged temperature, and the assumption that the bottom layer of the tank is at room temperature, an estimate for the heat conducted away through the bottom of the fluid cell can be established. This estimate turns out to be about 2·3 % of the total heat for a glass bottom. So about 97·7 % of the heat generated in the fluid leaves through the cooling plate.

The total heat input was varied between 25 W and 860 W. This corresponds to a voltage of between 50 V and 230 V to be applied between the electrodes. The average heat generation per unit volume and time was 0·017 to 0·58 cal cm^{-3} sec^{-1}.

The viscosity of zinc sulphate solution of density 1·05 g cm^{-3} was found to be about 20 % higher than that of pure water. An Ostwald viscometer was used for this measurement. The factor of 1·2 was taken into account in determining (7).

4. Evolution of the convection pattern

The purpose of this section is to describe the development of the convection pattern with time, which was not mentioned by Tritton & Zarraga, but emerged as a major feature of all experiments. As explained below, a time period of about 1 h following the application of voltage to the fluid is considered. The description applies essentially to a glass bottom for the shallow ($d = 0{\cdot}46$ cm) convection space and the Teflon layer only providing the insulation between the fluid and the cooling plate. However, the evolution under these conditions is typical. Some effects of changes in the setup on the convection will be mentioned explicitly. The change of the fluid-layer depth will be described separately in § 6.

An experiment is started at time $t = 0$ by applying a fixed voltage across the fluid. The current will rise for some time as the fluid heats up. When an equilibrium is reached between the rate of heat generation and the rate of heat loss through cooling the current will stabilize. Measured values of current I as a function of time t are shown in figure 5. The current is within 1 % at its final value after 10 min. This transient period depends strongly on the tank bottom and top materials. For instance, with the Plexiglass bottom the current reached its final state in only 2 min. A typical current-time curve for Plexiglass is shown by the dashed curve in figure 5.

The total time duration of each experiment was unexpectedly limited by undesired effects. After some time, during an experiment gas bubbles started to form at the electrodes. The size of these bubbles grew until, at high power levels after an hour, they reached a diameter of about 0·6 cm. They were mainly confined to an area within 1 cm of the electrodes, but the change in cross-section of the fluid in this area caused edge effects which extended visibly to about 4 cm from

the electrodes and were not negligible any more. So the duration of the experiments was usually limited to 1 h. The exact reason why these gas bubbles form is not known. Using distilled water and reasonably pure crystallized zinc sulphate to prepare the solution did not overcome the difficulties. Probably, hydrolysis of the water ($H_2O \rightarrow H^+ + OH^-$) contributed most to it. It may also be mentioned that, with stronger heating, air bubbles were gradually drawn into the convection space when the Plexiglass bottom was used figure 7 (*c*) (plate 2). This effect was caused by a mechanical warping of the Plexiglass due to heating. Therefore, most of the experiments were conducted with the glass bottom.

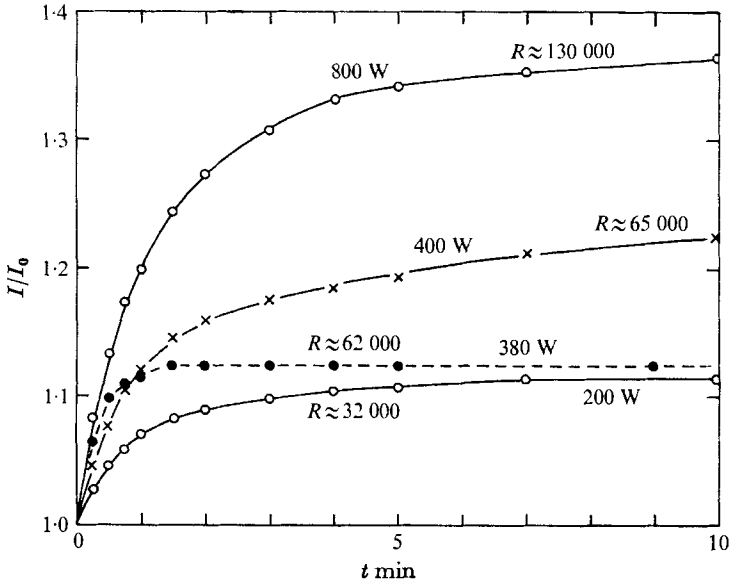

FIGURE 5. Current through the fluid as a function of time, for constant voltage. $T_c = 24$ °C, $d = 0{\cdot}46$ cm.

During an experiment, a visible cell pattern begins to emerge after about 2 or 3 min. This initial cell pattern is independent of the power level applied. It is always a more or less regular hexagonal cell pattern with an average cell diameter of approximately 10 mm. The fluid falls in the centre of the cells (down-hexagons). This latter feature persists throughout the further development of the pattern, except in the case of a cell breakup, which will be discussed further below.

As soon as the first pattern emerges, it starts changing. As time proceeds, the convection cells alter their position and grow in diameter. This growth is most dramatic at a Rayleigh number of $R \approx 3{\cdot}2 \times 10^4$, and is illustrated by figure 6 (plate 1), which presents photographs of the cell pattern as it appeared at various times. All photographs pertain to the same experiment with unchanged voltage, the only variable being time as indicated in the legend.

One could be tempted to argue that the growth of the cell size might be related to the increase in current, so that the growing heat input caused the growth in cell diameter. However, this argument does not provide a satisfactory explana-

tion for the following two reasons. First, the time scales do not coincide. While the current essentially has reached its final value after only 10 min, the diameter of the convection cells surprisingly keeps on growing, as is evident from figure 6. Secondly, the initial pattern does not depend on power at all. For example, the initial power of an experiment with $R \approx 13 \times 10^4$ is much higher than at $R \approx 3{\cdot}2 \times 10^4$; nevertheless, the cells of the initial pattern start with the same small diameter.

While at $R \approx 3{\cdot}2 \times 10^4$ the diameters of the convection cells do increase as described above, the developed cells keep their essentially hexagonal shape. This is not so at higher power levels. At an input of $R \approx 6{\cdot}5 \times 10^4$, or more, the cells tend to merge and form rolls, as shown in figure 7 (plate 2). The roll patterns were also more or less regular in shape. However, sharply established rolls were considerably less time dependent in size and location than hexagons. In fact, photographs taken at consecutive times yielded at least some indication that a perfect roll pattern could exist as a steady state. For a glass-bottom tank, rolls were usually well established within 25 min after the beginning of the experiment. This transition time appeared to be shorter for Plexiglass-bottom tanks.

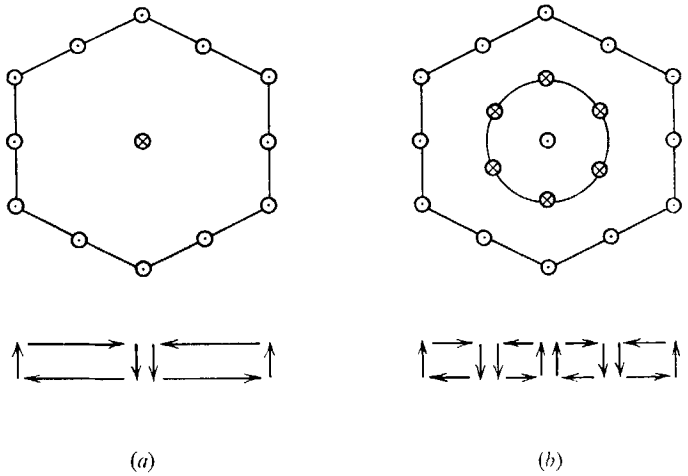

(*a*) (*b*)

FIGURE 8. Schematic breakup of regular flow pattern in a large hexagonal cell (d = 0·46 cm).

On the other hand, it remains very doubtful whether or not a true hexagonal pattern could exist as a steady state. The present observations did not support any such conclusion. Considering the fact that experiments with Bénard convection and Taylor vortices by Koschmieder (1969), Snyder (1969), and others, had to be conducted for 10 h, and more, one might dispute any steady-state validity of the present 1 h observations. However, most of the experiments were conducted at a power level far above the critical heating, so that at least steady-state symptoms could be expected within 1 h. Indeed, as was mentioned above, at higher power inputs, the occurring roll pattern displayed some stationary features with 25 min. For all power levels producing hexagonal patterns, no such

tendency of a steady-state development was visible. The cells continued changing for the full one-hour observation. On several occasions, sharp boundaries seemed to have evolved, but broke up again as time went on.

For example, for experiments with $R \approx 3{\cdot}2 \times 10^4$, it was observed on various occasions, that, in a particularly large cell, the fluid changed its characteristic flow behaviour. While normally the fluid descends in the centre, and ascends at the periphery of the cells, in these cases a flow pattern developed as shown in figure 8(*b*). The fluid now ascends at the cell centre, and an additional vertical flow is established between the centre and the periphery, which was not there before. The transition from the usual pattern of figure 8(*a*) to the pattern of figure 8(*b*) was observed only at power levels of $R \approx 3{\cdot}2 \times 10^4$ and $R \approx 4{\cdot}3 \times 10^4$. Cells, for which this transition was observed, had diameters clearly larger (about 33–35 mm) than the average diameter observed at that time. These large cells with inverted flows eventually broke up into several cells with normal flows.

In the absence of a clear steady state, especially the term 'hexagonal' pattern used here must be regarded in a rather wide sense. For the same reason, such hysteresis effects as those reported by Chen & Whitehead (1968), Krishnamurti (1968), Davis & Segel (1968), and Snyder (1969) could not be expected. Even in the case of more stationary rolls, if the voltage during an experiment with $R \approx 6{\cdot}5 \times 10^4$ was suddenly raised to a level corresponding to $R \approx 13 \times 10^4$, the roll diameter changed to the size that was normally obtained at that level (figures 7(*a*), (*b*), plate 2).

5. The flow pattern and its dependence on parameters

As described in § 4, the observed flow patterns are either more or less regular hexagons, or rolls depending on time and power level (figures 6, 7). The agreements that could be achieved with the experiments of Tritton & Zarraga are of the following qualitative nature: Perfectly regular hexagons were only occasionally observed, and only in isolated locations. When compared to the similar Bénard convection, a rather strong elongation of the cells was clearly visible. Finally, the direction of the motion within the cells is downward in the centre. Other qualitative and quantitative properties observed displayed deviations from the results of Tritton & Zarraga. The strong time dependence and limitation have been discussed in § 4.

The new experiments indicated that the channelled cooling device used by Tritton & Zarraga did not influence the convection pattern. Furthermore, the cell pattern remained independent of the direction of the cooling water, which was changed to flow parallel or normal to the electric current.

In agreement with Tritton & Zarraga, no striking influence of the direction of the electric current on the hexagonal pattern was immediately visible. Of course, this emphasizes the irregularities of the flow pattern, which was constantly changing. Assuming that a steady-state hexagonal pattern is possible, one ought to expect on physical grounds a hexagon arrangement aligned to the electric current, as sketched in figure 9. The cell-current alignment shown would accomplish the best electrical conduction and heating.

Indeed, a more careful look at the photographs of Tritton & Zarraga (especially their figures 4, 5), and at the present figures 6, 7 (*d*), easily convinces one that the hexagon-current alignment, sketched in figure 9, exists. In the case of the roll-type pattern, the co-orientation of the rolls with the electric current is most strikingly visible in Tritton & Zarraga's figures 7, 8, 11, and even more in the present figures 7 (*a*)–(*c*). To check this evidence further, the orientation of the fluid tank with respect to the cooling plate was changed by 90°, so that the water ran normal to the direction of the electric current. As anticipated, the rolls developed again parallel to the electric current. Tritton & Zarraga (1967, p. 24) discussed, and rejected, this effect on the basis of their observations. Judging from their published photographs, it seems that they never obtained a roll pattern as regularly developed as that shown in figures 7 (*a*)–(*c*), and, hence, they missed seeing the current-flow alignment.

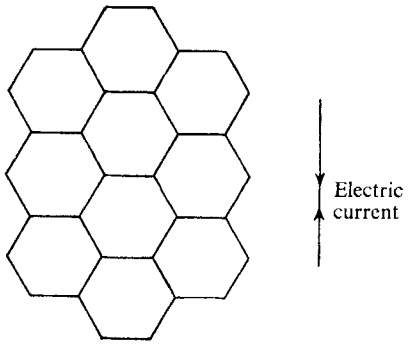

FIGURE 9. Scheme of regular hexagonal flow pattern perfectly aligned to the electric current.

The power input has a strong influence on the development of the hexagonal and roll patterns. Figure 10 shows average diameters $\bar{D}$ of hexagons and rolls as a function of time t and Rayleigh number R. Solid lines indicate hexagons, and dashed lines designate a domination of rolls. The average diameters shown were determined from many experiments. Individual cells differ from this average, as can be seen in figures 6, 7, which are typical. It is interesting to note that $\bar{D}$ is not a monotonic function of H. The hexagons in an experiment with $R \approx 3{\cdot}2 \times 10^4$ are more elongated than the rolls at $R \approx 6{\cdot}5 \times 10^4$, which is probably a consequence of their different geometrical meanings.

Another less essential discrepancy between the experiments of Tritton & Zarraga and the present ones becomes evident from figures 6, 7, 10. The former authors claim to have seen circulations of width (distance between up and down motions) up to five times the fluid-layer depth, which corresponds to a hexagon diameter of up to 44 mm. Figure 10 shows that the mean diameter of the present cells was less than 29 mm, and at no time were cell diameters larger than 35 mm observed.

Experiments by Koschmieder (1966) and others revealed a dilation of convection cells if the fluid layer was covered with a plate of smaller thermal conductivity. Remembering that the present experiments were conducted with

a glass-bottom tank of thermal conductivity 0·0023 cal sec^{-1} cm^{-1} °C^{-1}, while Tritton & Zarraga used Perspex of considerably smaller conductivity one might even anticipate a still wider gap between the results. To investigate this matter, which has not been studied before, the glass was replaced by Plexiglass, which has the same chemical composition as Perspex, and hence comparable thermal conductivity (of about 0·0005 cal sec^{-1} cm^{-1} °C^{-1}). The cell diameters were found to be generally the same as obtained with the glass bottom. Some experiments at lower power levels up to $R \approx 6{\cdot}5 \times 10^4$ indicated a slight enlargement of the cells. Only at the power level of $R \approx 11{\cdot}3 \times 10^4$ (figure 7 (*a*)) did the rolls appear to be slightly smaller.

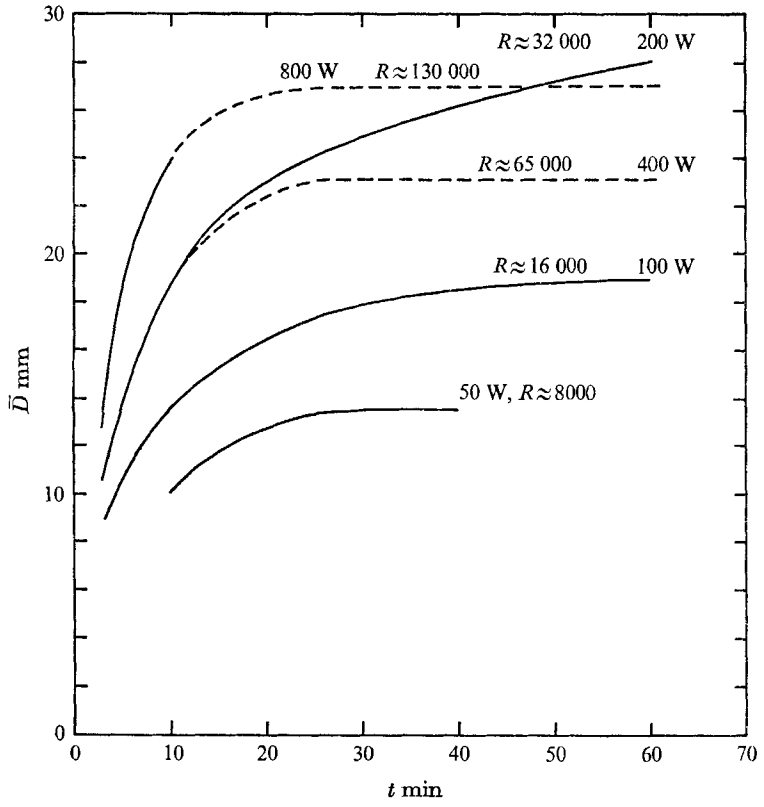

FIGURE 10. Average diameters $\bar{D}$ of hexagonal cells (——) and rolls (– – – –) as a function of time and total heat input for a glass bottom (d = 0·46 cm). T_c = 24 °C.

What, then, is the cause of these minor differences between the two experiments? The only remaining factor appeared to be the difference in the coating of the cooling plates on top of the convecting fluid. The amount of thermal insulation provided by the Teflon layer can be estimated from its thermal conductivity of 0·0006 cal sec^{-1} cm^{-1} °C^{-1}. The result is that a temperature difference of about 0·0052 °C per watt of total heat input will build up across the Teflon layer. This amount is not negligible compared with the temperature difference in the fluid that was discussed in § 3.

In order to investigate the influence of the Teflon coating experimentally an additional insulation was added. Between one and three layers of polyester film tape of 0·1 mm thickness were used. In these experiments, the patterns did not develop as sharply as they did without the additional insulation. Little irregularities were noticeable in the pattern development where the tape strips joined, although the tape had been put on with great care.

Thus, no quantitative information was derived from the observations. However, two general trends could be clearly recognized. The added insulation impedes the formation of rolls. No clear roll pattern was found to evolve for any experiment with various heat inputs up to $R \approx 13 \times 10^4$ and various insulating layers. This effect was not due to any striation introduced by the tape strips. The same results were obtained whether the striation was oriented parallel or vertical to the electric current. The diameters of the cells obtained were larger than those which would have developed without the added insulation at the same power level. For example, cell diameters of 30 mm were observed at $R \approx 6{\cdot}5 \times 10^4$ with two layers of tape, using the Plexiglass bottom. The usual rolls at this power input had a diameter of about 27 mm.

Tritton & Zarraga did not give any thermal specifications of the polyurethane lacquer and paint coatings of their cooling plate. Nevertheless, the observations mentioned above do indicate that the discrepancies between the two experiments could be explained by the different coating of the cooling plates, at least to some extent. Moreover, a closer evaluation of the published photographs of Tritton & Zarraga yields only a maximum average cell diameter of about 37 mm instead of the claimed 44 mm.

In view of the investigations by Segel (1969) and Snyder (1969), the question of boundary effects was also tested by placing a strip of lucite into the fluid tank. The tank width was subdivided into two sections with a ratio of 2:1. The patterns in the smaller sections displayed no visible differences from those observed without the subdivision (figure 7 (*d*)). This result justifies the conclusion that boundary effects were negligible in the described experiments.

A final equipment variable is the absolute temperature T_c of the cooling water. Experiments with $R \approx 13 \times 10^4$ were made at cooling temperatures of 12 °C, 24 °C, and 32 °C. The differences in the results were within the range of deviations observed between identical experiments. This result is somewhat surprising, since both the viscosity and the coefficient of thermal expansion are strongly dependent on the temperature variation generated.

6. Summary and conclusions

As described in §§ 4 and 5 the new experiments with fluid layers of the shallow depth $d = 0{\cdot}46$ cm essentially confirmed the observations by Tritton & Zarraga with respect to cell form, cell diameter, and direction of circulation. Differences in the roll development and cell dilation at higher Rayleigh numbers could be attributed to some extent to the differences in the thermal properties of the electrical insulation of the cooling plate. While this paper was being published, D. J. Tritton (private communication) reported results of renewed experiments

by T. Hooper. According to this report, the dilation of the cell diameter at higher Rayleigh numbers is in full agreement with the present observations.

Extensive tests demonstrated convincingly that the convection currents are only very little, if at all, influenced by the temperature and flow direction of the cooling water, the thermal properties of the bottom plate, and the distance of the side walls. The thermal properties of the cooling plate showed some effect, but could almost definitely be excluded as the cause of the strong flattening of the cells. The new experiments by Tritton and Hooper appear to have also confirmed those results.

What, then, is the source of the strong dilation of the cellular flow? The answer to this fundamental questions can be derived from the following flow features: The new experiments revealed a clear co-orientation between the flow and the electric current which was also recognizable in the old experiments. Independent of the Rayleigh number, all experiments started with a small, more or less regular hexagonal pattern, which grew in size, and changed its shape and location far beyond the time at which the electric current had reached its final value. While roll patterns at large Rayleigh numbers appeared to attain a steady state, hexagonal cells remained time dependent with respect to irregular shape and location. In extremely large hexagons, the breakup was observed to start with a reversed flow in the centre of the cell. As described by Tritton & Zarraga, in the transition régime between hexagonal and roll patterns, a sort of rectangular roll pattern appeared, where the roll walls in the direction of the electric current became much stronger than the crossing walls (figure 7 (*b*)).

It seems very difficult to explain the observations collected above by a uniform internal heating, or by any temperature-dependent fluid property, with the exception of electric conductivity (equation (3)). In fact, one can argue on physical grounds that the direction-dependent electrolytic heating is the cause of the build-up and tear-down sequence displayed by the hexagonal motion. This self-destroying feature will be greatly reduced by the strong dilation of the cells. Having augmented the equations of motion with a direction–dependent heat source (equation (2)), it was possible to compute solutions which can, indeed, explain the mechanism behind all the observed flow properties. Details of this investigation will be presented in a forthcoming paper.

In this connexion, it may be mentioned that Tritton (private communication) also reported new improved calculations of Thirlby (1971). Again, the theory of Thirlby (1971) predicts no drastic dilation of the cells under uniform heating. This, too, is in agreement with the authors' theoretical investigations.

After the source of the peculiar properties of the convection currents, discovered by Tritton & Zarraga, had been traced to the temperature–dependent electric conductivity, it was suggested by one of the referees that this effect should be diminished in a thicker fluid layer. If one defines the Rayleigh number R (equation (1)) on the basis of a properly defined characteristic temperature T_c, one has $R \sim T_c d^3$. Hence, by increasing the depth of the fluid layer, e.g. from d to $2d$, the characteristic temperature can be dropped from T_c to $T_c/8$ without changing the Rayleigh number R. At the same time, the magnitude of (βT_c) in the electric conductivity (equation (3)) is diminished to $(\beta T_c)/8$. Thus, a drastic

reduction of the effect of the electric current might be anticipated. However, one must remember that the increase of the fluid-layer depth destabilizes the fluid, i.e. a smaller temperature difference should produce the same effect. Since the term (βT_c) enters in the equations of motion in a highly non-linear manner, numerical calculations showed that noticeable differences between convection in thin and thick layers can, indeed, be expected.

In fact, experiments with thicker fluid layers at high Rayleigh numbers have already been made by Tritton & Zarraga. According to their report (p. 28), a 'perturbing' reduction of the cell dilation was visible. A more careful evaluation of their published photographs shows a flattening of the cells by a factor of about 3, which is very close to the present experiments with the thin fluid layer.

In order to remove any uncertainties, it was decided to repeat the experiments with the Plexiglass-bottom tank, the walls of which were raised to 0·90 cm, to achieve an increase of the fluid-layer thickness from $d = 0{\cdot}46$ cm to $2d = 0{\cdot}92$ cm. Otherwise, the apparatus remained unchanged and the identical fluid was used. As anticipated, the following observations were made:

(i) The flow development needed about twice as much time as before, which is in agreement with the characteristic velocity scale $V_c \sim 1/d$.

(ii) The convection could be observed for over 3 h without any bubble disturbances.

(iii) As before, more or less regular hexagonal and roll patterns evolved, but the roll currents were less pronounced (figure 11, plate 3).

(iv) For Rayleigh numbers up to $R \approx 3{\cdot}2 \times 10^4$, the convection flow displayed no clear evolution stages and settled slowly on a hexagonal pattern which appeared to remain steady. At larger Rayleigh numbers up to $R \approx 26 \times 10^4$, the convection again went through evolution stages before it settled in a less regular roll pattern.

(v) The hexagonal pattern up to $R \approx 3{\cdot}2 \times 10^4$ revealed no detectable co-orientation with the electric current (figure 11 (*a*)). The roll pattern up to $R \approx 26 \times 10^4$ remained aligned to the electric current.

(vi) Relative to the most critical wavelength $\lambda_c = 2\pi d/a_c$ ($a_c \approx 2{\cdot}63$) determined by Roberts (1967) under ideal internal heating conditions, the elongation of the cell diameters ($D_c = 2\lambda_c/\sqrt{3}$ for hexagons, $D_c = \lambda_c$ for rolls) was found to be as in table 1.

R / d	$1{\cdot}6 \times 10^4$	$3{\cdot}2 \times 10^4$	13×10^4 (Rolls)
0·46	50 %	128 %	145 %
0·92	20 %	45 %	120 %

TABLE 1. Elongation of cell diameters D relative to most critical theoretical values D_c at various Rayleigh numbers R and fluid depths d

Based on these findings one can conclude that the observed strong dilation of the convection cells is essentially caused by the uneven electric heating. If one eliminates this cause (i.e. the temperature-dependent electric conductivity), it is

probable that no great differences between convection due to internal heating and that due to external heating will emerge. Furthermore, it is not unlikely that a satisfactory agreement between experiments and theory can be restored either by using more ideal materials or by incorporating their characteristics in a proper theory.

The authors thank Dr D. J. Tritton for communicating to them unpublished results of new experimental and theoretical investigations of the problem, which were conducted by him and his student Mr T. Hooper, and by Prof. P. H. Roberts and his colleague Mr R. Thirlby. The idea of increasing the fluid-layer depth, which was suggested by one of the referees, is also gratefully acknowledged.

REFERENCES

BUSSE, F. H. 1962 Dissertation, University of Munich. (Trans. S. H. Davis, *Rand Rept.* LT-66-19. Santa Monica, Calif.: Rand Corp.)

CHEN, M. M. & WHITEHEAD, J. A. 1968 *J. Fluid Mech.* **31**, 1.

DAVEY, A., DIPRIMA, R. C. & STUART, J. T. 1968 *J. Fluid Mech.* **31**, 17.

DAVIS, S. H. & SEGEL, L. A. 1968 *Phys. Fluids*, **11**, 470.

FIFE, P. C. & JOSEPH, D. D. 1969 *Arch. Rat. Mech. Anal.* **33**, 116.

JOSEPH, D. D. & SHIR, C. C. 1966 *J. Fluid Mech.* **26**, 753.

KOSCHMIEDER, E. L. 1966 *Beitr. Phys. Atmos.* **39**, 1.

KOSCHMIEDER, E. L. 1969 *J. Fluid Mech.* **35**, 527.

KRISHNAMURTI, R. 1968 *J. Fluid Mech.* **33**, 445, 457.

NIELD, D. A. 1968 *J. Fluid Mech.* **32**, 393.

PALM, E. 1960 *J. Fluid Mech.* **8**, 183.

ROBERTS, P. H. 1966 On nonlinear Bénard convection. *Non-equilibrium Thermodynamics, Variational Techniques and Stability* (ed. R. J. Donnelly, R. Herman & I. Prigogine). University of Chicago Press.

ROBERTS, P. H. 1967 *J. Fluid Mech.* **30**, 33.

SCHLÜTER, A., LORTZ, D. & BUSSE, F. H. 1965 *J. Fluid Mech.* **23**, 129.

SEGEL, L. A. 1965 *J. Fluid Mech.* **21**, 359.

SEGEL, L. A. 1969 *J. Fluid Mech.* **38**, 203.

SNYDER, H. A. 1969 *J. Fluid Mech.* **35**, 273, 337.

SOMERSCALES, E. F. C. & DOUGHERTY, T. S. 1970 *J. Fluid Mech.* **42**, 755.

SOMERSCALES, E. F. C. & DROPKIN, D. 1966 *Int. J. Heat Mass Transfer*, **9**, 1189.

THIRLBY, R. 1971 *J. Fluid Mech.* **44**, 673.

TRITTON, D. J. & ZARRAGA, M. N. 1967 *J. Fluid Mech.* **30**, 21.

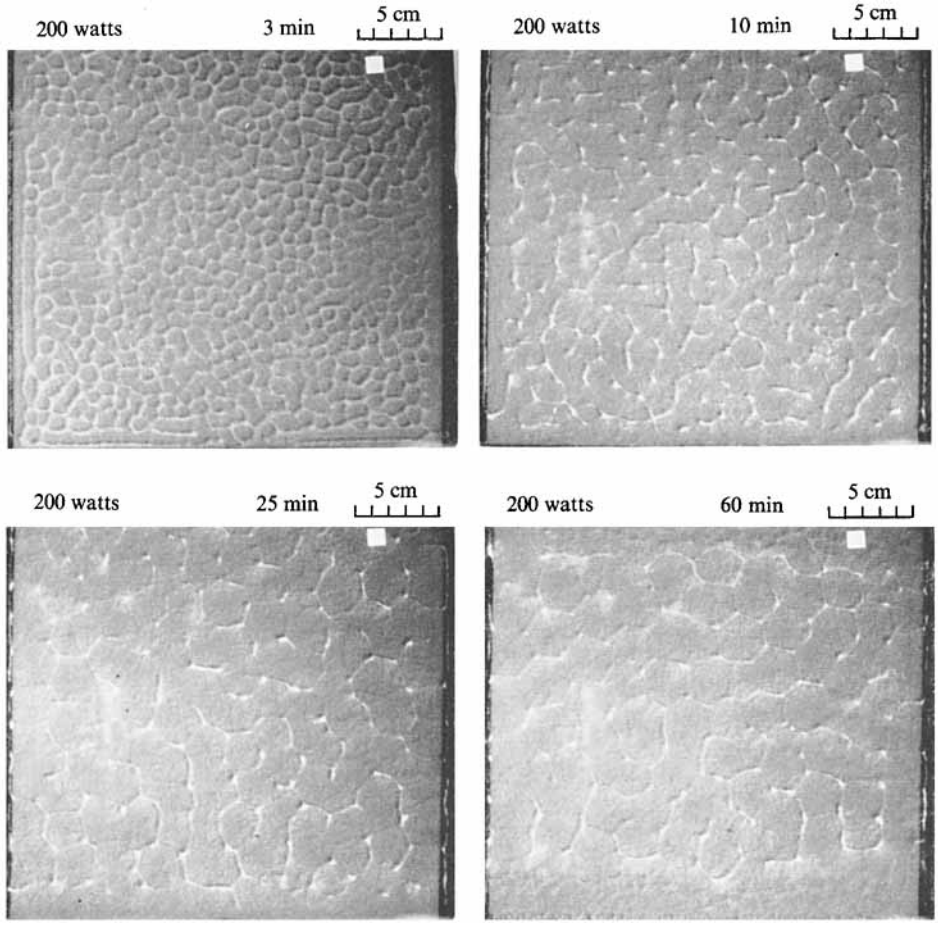

FIGURE 6. Convection pattern at various times after $t = 0$. $R \approx 3{\cdot}2 \times 10^4$, $T_c = 24$ °C, glass bottom, $d = 0{\cdot}46$ cm. Electric current alternating from top to bottom of page.

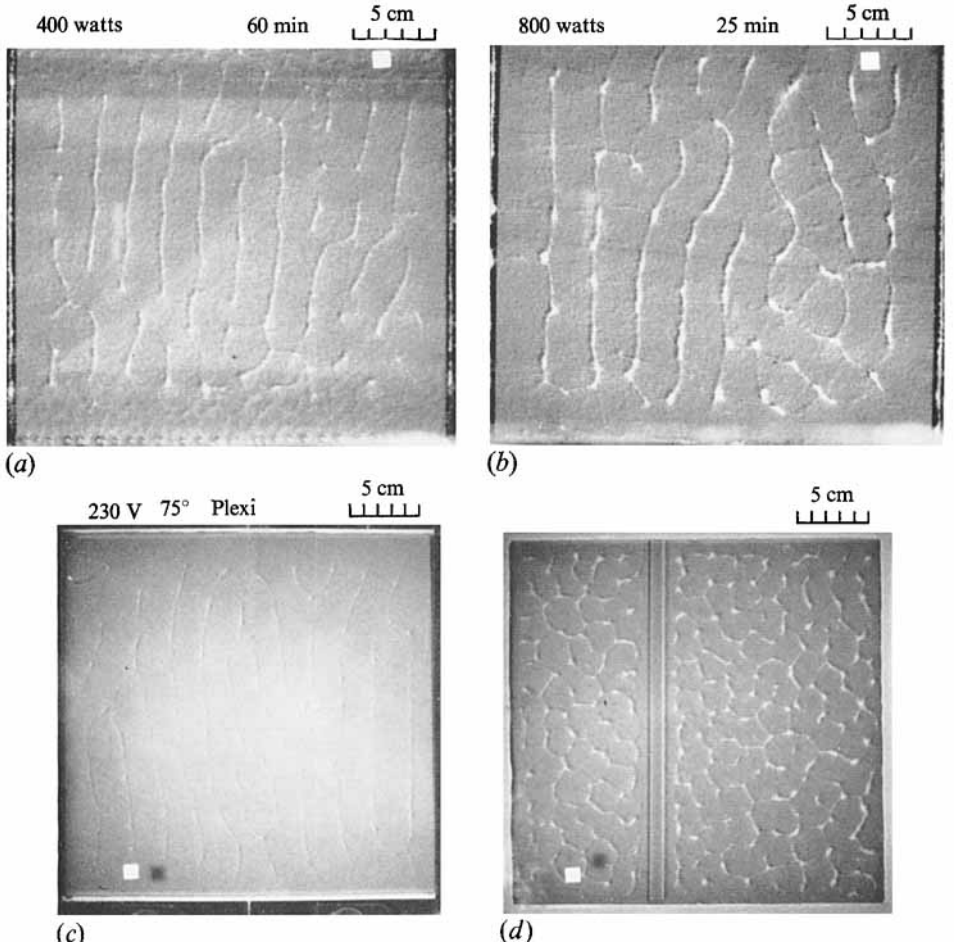

FIGURE 7. Photographs of convection patterns illustrating the influence of various parameters. (*a*) Roll pattern at $R \approx 6{\cdot}5 \times 10^4$, glass bottom; (*b*) roll pattern at $R \approx 13 \times 10^4$, glass bottom. (*c*) Roll pattern at $R \approx 11{\cdot}3 \times 10^4$, Plexiglass bottom. ($t = 16$ min). (*d*) Effect of additional boundary. $R \approx 3{\cdot}2 \times 10^4$, $t = 20$ min glass bottom. For all photographs, $T_c = 24$ °C, $d = 0{\cdot}46$ cm. Electric current alternating from top to bottom of page.

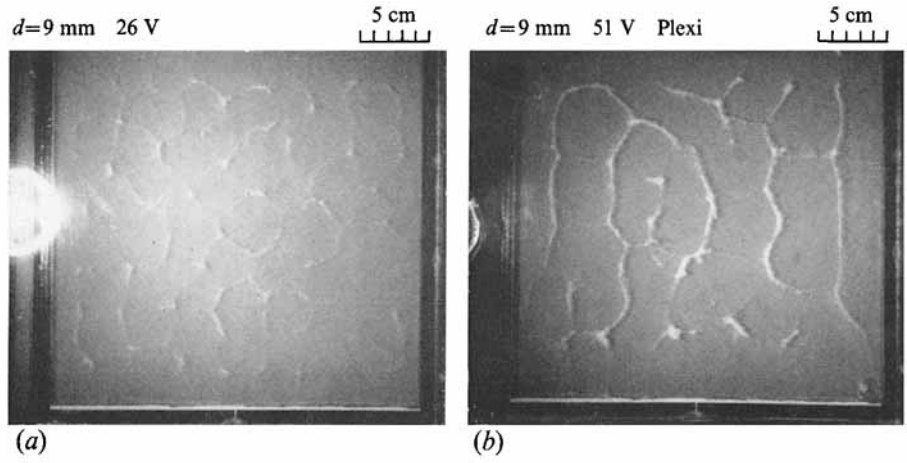

FIGURE 11. Photographs of convection at (*a*) $R \approx 3{\cdot}2 \times 10^4$, (*b*) $R \approx 13 \times 10^4$. Plexiglass bottom, $d = 0{\cdot}92$ cm, $t = 120$ min.